https://doi.org/10.46813/2022-137-147

COMPARISON OF CORROSION OF ALUMINUM-BASED ALLOYS FORMING DECAGONAL QUASICRYSTALS IN NaCl SOLUTION

V.A. Polonskyy, O.V. Sukhova
The Oles' Honchar Dnipro National University, Dnipro, Ukraine
E-mail: sukhovaya@ukr.net

In this work corrosion behavior of the $Al_{72}Co_{18}Ni_{10}$, $Al_{65}Co_{20}Cu_{15}$, and $Al_{72}Fe_{15}Ni_{13}$ alloys forming decagonal quasicrystalline phases was tested in the neutral NaCl solution (pH = 7) which allows a comparison of their corrosion resistance under conditions comparable to application in marine climate. The microstructure of the alloys was studied by quantitative metallographic, X-ray, scanning electron microscopic, and energy dispersive analyses. The corrosion properties were determined by gravimetric and potentiodynamic methods. The $Al_{65}Co_{20}Cu_{15}$ and $Al_{72}Fe_{15}Ni_{13}$ alloys have been established to corrode in the sodium chloride solution more strongly than the $Al_{72}Co_{18}Ni_{10}$ alloy. The corrosion that proceeds under electrochemical mechanism is accompanied by the formation of passive layer on the surface that retards further dissolution in the saline solution after 3–4 days of testing. Scanning electron microscopy shows the marks of pitting corrosion. The pits appear mostly where flaws and boundaries of iron- or aluminum-rich crystalline phases are located. Their quantity and size are lesser on the surface of the $Al_{72}Co_{18}Ni_{10}$ alloy since Co and Ni in its composition are rate determining for the corrosion processes. This alloy may be recommended as starting material for plasma-spayed coatings working in marine climate.

PACS: 61.50.Lt, 61.72.Ff, 62.23.Pq, 68.35 Fx, 68.35.Np, 81.05.Je, 81.40.Cd

INTRODUCTION

For many applications, susceptibility to corrosion in marine environment is of greatest importance. Most metals and alloys inevitably corrode because seawater is highly corrosive. To ensure long-term safe operation of equipment, reasonable selection of materials is the most important aspect. Appropriate combinations of alloy constituents obviously promote corrosion resistance. It is necessary to consider the materials structure, properties, and changes during use process [1].

The unique surface properties of quasicrystalline alloys, such as good corrosion and wear resistance, high hardness and low friction coefficient, make them promising materials to many practical purposes [2, 3]. In anticorrosion applications, Al-Cu-Fe alloys are the most often utilized quasicrystalline materials [4]. These alloys form icosahedral quasicrystalline phase, aperiodic in three dimensions, after slow solidification [5–7]. They are generally used in the form of thick coatings produced by plasma spraying [8].

Few works have been published on the corrosion behavior of the Al-Cu-Fe alloys in the sodium chloride aqueous media [9, 10]. A homogeneous dissolution of the alloys in the NaCl solution proceeds independent of alloy composition. A dissolution rate is determined by the volume fraction of Cu-rich phases present in the structure. The dissolution is accompanied by the redeposition of copper. It has been found that the corrosion properties of the Al-Cu-Fe alloys are affected rather by their chemical composition than crystallographic structure. At that, iron is considered a weak component in the corrosion of the alloys in the sodium chloride solutions [11].

Therefore, conventionally solidified quasicrystalline alloys of Al-Cu-Co and Al-Co-Ni systems may be regarded as better candidates for application in marine environment. These alloys are known to yield quasicrystalline decagonal phase that features aperiodic crystallographic order in two dimensions and periodic order along the third dimension [12–17]. Decagonal quasicrystals are also found in the Al-Ni-Fe alloy system [17, 18]. The combination of two different crystallographic orders sets decagonal quasicrystals apart from icosahedral quasicrystals [19, 20]. Their properties exhibit a qualitative difference from those of the icosahedral materials [21–27]. It may relate to corrosion properties as well. Besides, most alloys are also known to acquire enhanced performance characteristics due to rapid cooling during plasma atomization process [28–31].

Thus, Al-based alloys forming decagonal quasicrystalline phases show significant potential for use as plasma-sprayed coatings for practical applications in marine climate. But, in the literature, their corrosion behavior in sodium chloride aqueous solutions has not been comprehensively studied. Therefore, the purpose of this work is to compare the corrosion properties of decagonal quasicrystals formed in the Al-Co-Ni, Al-Cu-Co, and Al-Ni-Fe alloy systems in order to choose appropriate composition of starting materials for plasma-sprayed coatings.

1. MATERIALS AND METHODS

The quasicrystalline $Al_{72}Co_{18}Ni_{10}$, $Al_{65}Co_{20}Cu_{15}$, and $Al_{72}Fe_{15}Ni_{13}$ alloys were prepared of high purity components (99.99%) put in a graphite crucible and melted using Tamman furnace. The samples were cooled at a rate of 5 K/s. The compositions of the alloys were set close to the compositional range where the decagonal phase had been firstly obtained. The average chemical composition of the alloys was checked by atomic absorption spectroscopy method with Sprut СЕФ-01-М device. The relative precision of the measurements was better than ± 1 at.%. The alloys were examined by Neophot and GX-51 light-optical microscopes (OM). Quantitative metallography was

carried out with structural analyzer Epiquant. The alloys were also studied by powder X-ray diffraction (XRD) using ДРОН-УМ-1 diffractometer with CuK_α radiation. The phase compositions were determined in a scanning electron microscope РЭММА 102-02 (SEM) by energy-dispersive X-ray analysis on unetched cross-sections.

Corrosion behavior was investigated in the NaCl aqueous solution (pH = 7) at the temperature of (293±2) K. Corrosion immersion tests for 1…8 days were carried out with specimens 3×0.5 cm in size. The specimens were fully immersed in the saline solution. The corroded surface morphology was examined using a scanning electron microscope РЭМ-106И. Corrosion rates were determined from mass change measurements as a function of exposure time to a corrosive environment and calculated using formula given in [32].

Electrochemical measurements were performed using a computer-controlled system including ПИ-50-1 potentiostat and ПР-8 programmer using three-electrode electrolytic cell. The analyzed sample served as working electrode, a platinum plate – as counter electrode, and silver chloride electrode – as reference electrode. A surface of 1 cm^2 was exposed to the solution for all electrochemical experiments. To avoid contamination of the solution by chloride ions, the reference electrode was in contact with the working electrode through an electrolyte bridge. Saline solution was freshly prepared from distilled water and pure grade chemicals. The solution was exchanged after each measurement to avoid contamination of soluble species. Potentiodynamic measurements were carried out by scanning the potential in the positive or negative direction with a scan rate of 1 mV/s until a current limit in the milliampere range was reached. All samples, immersed into saline solution, were initially stabilized at a free corrosion potential prior to conducting potentiodynamic scans. Corrosion current density was obtained by extrapolating the linear portion of the anodic and cathodic branches of the polarization curves to free corrosion potential.

2. RESULTS AND DISCUSSION

The structure of the $Al_{72}Co_{18}Ni_{10}$ alloy is composed of primary quasicrystalline decagonal D-phase of the stoichiometric composition $Al_{69}Co_{21}Ni_{10}$ and crystalline $Al_9(Co, Ni)_2$ phase that solidifies via peritectic reaction between the D-phase and the liquid (Fig. 1). The volume fraction of D-quasicrystals is about 60 vol.% of a total alloy volume [33]. They are sized from 50 to 80 μm due to differing local growth conditions.

The $Al_{65}Co_{20}Cu_{15}$ alloy exhibits three-phase structure consisting of quasicrystalline decagonal D-phase of the stochiometric composition $Al_{65}Co_{20}Cu_{15}$ and crystalline phases of $Al_4(Co, Cu)_3$ and $Al_3(Cu, Co)_2$ (Fig. 2). Quasicrystalline D-phase takes about 65 vol.% of a total alloy volume [34]. The size of quasicrystals varies from 40 to 60 μm. The solidification of the D-phase proceeds via a peritectic reaction, in which the primary $Al_4(Co, Cu)_3$ crystals are surrounded by the quasicrystalline shells. Afterwards $Al_3(Cu, Co)_2$ phase solidifies.

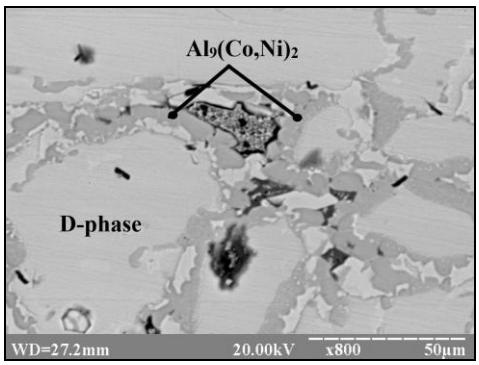

a

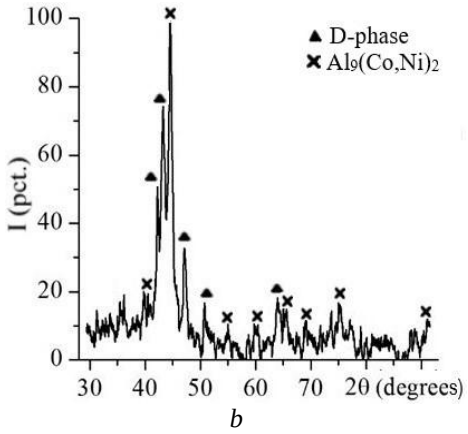

b

Fig. 1. The $Al_{72}Co_{18}Ni_{10}$ alloy: a – SEM image; b – XRD pattern

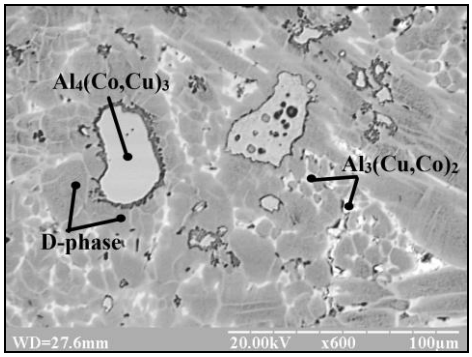

a

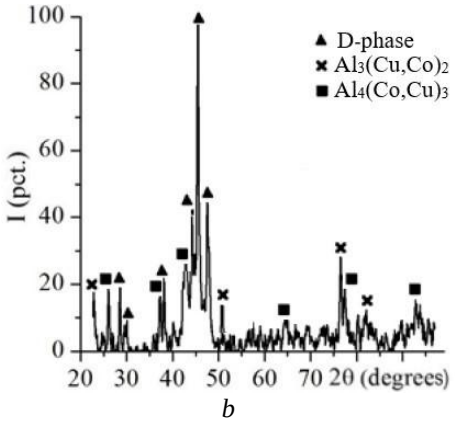

b

Fig. 2. The $Al_{65}Co_{20}Cu_{15}$ alloy: a – SEM image; b – XRD pattern

The $Al_{72}Fe_{15}Ni_{13}$ alloy consists of primary Al_5FeNi crystals separated by secondary quasicrystalline decagonal D-phase (Fig. 3). The estimation of D-phase stochiometric composition gives $Al_{72}Ni_{17}Fe_{11}$. The volume fraction of D-phase reaches 30 vol.% of a total alloy volume [35].

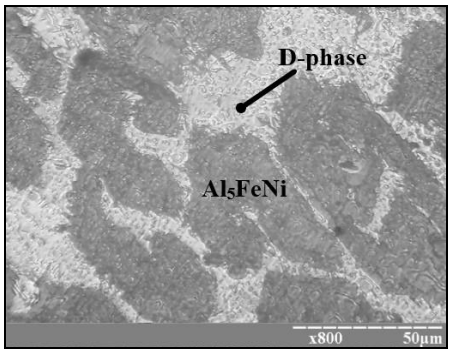

a

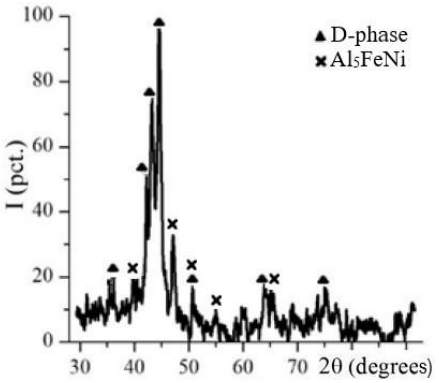

b

Fig. 3. The $Al_{72}Fe_{15}Ni_{13}$ alloy: a – OM image; b – XRD pattern

When subjected to corrosion in the aqueous NaCl solution (pH = 7), the studied $Al_{72}Co_{18}Ni_{10}$ alloy does not noticeably corrode. Gravimetric measurements show that, at first, specific change in the mass gradually increases up to 4.3 g/m^2 for 4 days and then stabilizes (Table 1). The greatest mass gain is revealed after 2 days of testing.

Table 1

Specific mass change, g/m^2, of the investigated alloys in the sodium chloride solution (pH = 7)

Alloy	Exposure time, days				
	1	2	3	4	8
$Al_{72}Co_{18}Ni_{10}$	0.00	1.2	3.0	4.3	4.3
$Al_{65}Co_{20}Cu_{15}$	1.2	4.8	6.5	7.2	8.0
$Al_{72}Fe_{15}Ni_{13}$	0.0	1.4	3.3	4.2	4.5

Among the investigated quasicrystalline Al-based alloys, the $Al_{65}Co_{20}Cu_{15}$ alloy is found to have the greatest change in mass, compared to the other alloys (see Table 1). After 8 days of the tests in the aqueous sodium chloride solution, the specific mass change of the $Al_{65}Co_{20}Cu_{15}$ alloy amounts to 8.0 g/m^2. The mass of specimens gradually increases, especially after 1 day of treatment. Then, after 3 days of exposure to the NaCl solution, the mass of specimens changes to a much lesser extent.

The mass gain of the $Al_{72}Fe_{15}Ni_{13}$ alloy in the NaCl solution is comparable to that of the $Al_{72}Co_{18}Ni_{10}$ alloy (see Table 1). The specific mass change of the alloy reaches the value of 4.5 g/m^2 after 8 days of testing. The mass mainly increases after 2 days of staying in the solution.

Thus, gravimetric measurements evidence that the mass of the analyzed alloys remains nearly unchanged after 3–4 days of test which reduces the corrosion rates to negligible levels (Table 2). This indicates that the adherent passive films consisted of corrosion products are formed during this time. The films are registered visually as surface darkening that shows no color change of the surface with immersion duration. Their presence obviously suppresses the attack. Meanwhile, color and transparency of working solution do not practically change. The $Al_{72}Co_{18}Ni_{10}$ and $Al_{72}Fe_{15}Ni_{13}$ alloys are found to corrode in the neutral solution at the lowest rate (see Table 2). So, for the analyzed samples, behavior is consistent with the formation of protective passive layers.

Table 2

Corrosion properties of the investigated alloys in the sodium chloride solution (pH = 7)

Alloy	Corrosion rate, g/(m^2·h)	Free corrosion potential, V	Corrosion current density, mA/cm^2
$Al_{72}Co_{18}Ni_{10}$	0.02	–0.40	0.12
$Al_{65}Co_{20}Cu_{15}$	0.04	–0.43	0.18
$Al_{72}Fe_{15}Ni_{13}$	0.02	–0.55	0.20

Cyclic voltammetry measurements of the investigated alloys are in good agreement with gravimetric results. Polarization curves show that the potentials of the alloys increase quickly towards less negative values during first 5…7 min and then stabilize at the values of free corrosion potential that is a good indication of the alloys' tendency to corrode in the NaCl solution (see Table 2). Such behavior is indicative of a typical passive oxide film present on the surface of the alloys. A steady potential testifies that the passivation film build-up in the NaCl solution remains rather protective.

The recorded values reveal that a free corrosion potential of the $Al_{72}Co_{18}Ni_{10}$ alloy stabilizes at the lowest value (see Table 2), as compared with that of the other alloys, which indicates more passive state of its surface. This alloy exhibits stronger propensity to form passivating oxide layers with higher stability. On the contrary, the $Al_{72}Fe_{15}Ni_{13}$ alloy presents the highest free corrosion potential, probably due to the presence of iron in its composition. At that, while staying in the NaCl solution, the $Al_{72}Fe_{15}Ni_{13}$ alloy exhibits values of mass change close to those of the $Al_{72}Co_{18}Ni_{10}$ alloy. This controversy may be associated with unstable dissolution of the passive film formed on the surface of the $Al_{72}Fe_{15}Ni_{13}$ alloy. And, ultimately, the film on the surface of the $Al_{65}Co_{20}Cu_{15}$ alloy has the largest thickness as compared with the other alloys. Considering that the value of free corrosion potential for the $Al_{65}Co_{20}Cu_{15}$ alloy is a little higher than that for the $Al_{72}Co_{18}Ni_{10}$ alloy, it may be concluded that the film on

its surface is more porous and retards alloy's dissolution to a lesser extent. That is why, oxygen penetrates into pores of the passivation film and causes its further growth. As a result, the $Al_{65}Co_{20}Cu_{15}$ alloy exposed to the saline solution has the largest mass gain and exhibits the highest value of corrosion rate of all the investigated alloys.

Polarization measurements also evidence that corrosion of the alloys in the sodium chloride solution is typical to processes with oxygen depolarization. Fig. 4 illustrates the polarization curves recorded with periodic sweeping the potential in the opposite directions. During testing, as the potential departs from a free corrosion potential to more positive values, the anodic current density rises continuously. At potential of ~ -0.3 V, anodic current increases sharply which may relate to active dissolution of alloy components. When direction of potential scan is reversed, the null value of current density is reached at potential of -0.86 V for the $Al_{72}Co_{18}Ni_{10}$ alloy (see Fig. 4,a); -0.87 V for the $Al_{65}Co_{20}Cu_{15}$ alloy (see Fig. 4,b), and -0.88 V for the $Al_{72}Fe_{15}Ni_{13}$ alloy (see Fig. 4,c).

At potentials more negative than -1.0 V, a cathodic current density increases which relates to active hydrogen evolution. Polarization curves exhibit a stable electrochemical passivity region at the next cycle of a potential scan where the current density is independent of the applied potential. For the $Al_{72}Fe_{15}Ni_{13}$ alloy, this region extends from -1.0 to -0.5 V. For the $Al_{72}Co_{18}Ni_{10}$ and $Al_{65}Co_{20}Cu_{15}$ alloys, passivity regions are of similar size from -1.0 to -0.4 V which evidences that these alloys are less susceptible to corrosion in the NaCl solution, compared to the $Al_{72}Fe_{15}Ni_{13}$ alloy. Due to inhibition of anodic processes, the broader passive range of the $Al_{72}Co_{18}Ni_{10}$ and $Al_{65}Co_{20}Cu_{15}$ alloys also indicates higher stability of passive films on the surface.

Thus, polarization curves show that the $Al_{72}Fe_{15}Ni_{13}$ alloy is the most susceptible to corrosion. The made conclusion is consistent with values of corrosion current density exhibited by potentiodynamic curves (see Table 2). Obviously, presence of Fe in the $Al_{72}Fe_{15}Ni_{13}$ alloy is responsible for the highest value of current density that does not approach zero as easily as that of the other alloys. Such behavior can be caused by the effect of the dissolution of the passive film formed on the surface. This would suggest that the Fe content in the alloy is an important factor influencing the overall corrosion properties due to formation of less stable film. On the contrary, the lowest current density for the $Al_{72}Co_{18}Ni_{10}$ alloy reveals highest stability of passive film. It may be due to the presence of inhibiting constituents like Co and Ni. Compared with the $Al_{72}Co_{18}Ni_{10}$ alloy, the higher value of current density for the $Al_{65}Co_{20}Cu_{15}$ alloy indicates the higher corrosion susceptibility due to the formation of porous protective film.

So, the corrosion of the studied alloys in the neutral NaCl solution occurs by electrochemical mechanism that dictates the ultimate corrosion rate. No active dissolution region is apparent, thus indicating that the surface of the alloys is covered with passive oxide layer that remains most stable for the $Al_{72}Co_{18}Ni_{10}$ alloy. This may be attributed to the better transition of the alloy to passive state. As a result, the $Al_{72}Co_{18}Ni_{10}$ alloy is the most corrosion resistant in the saline environment.

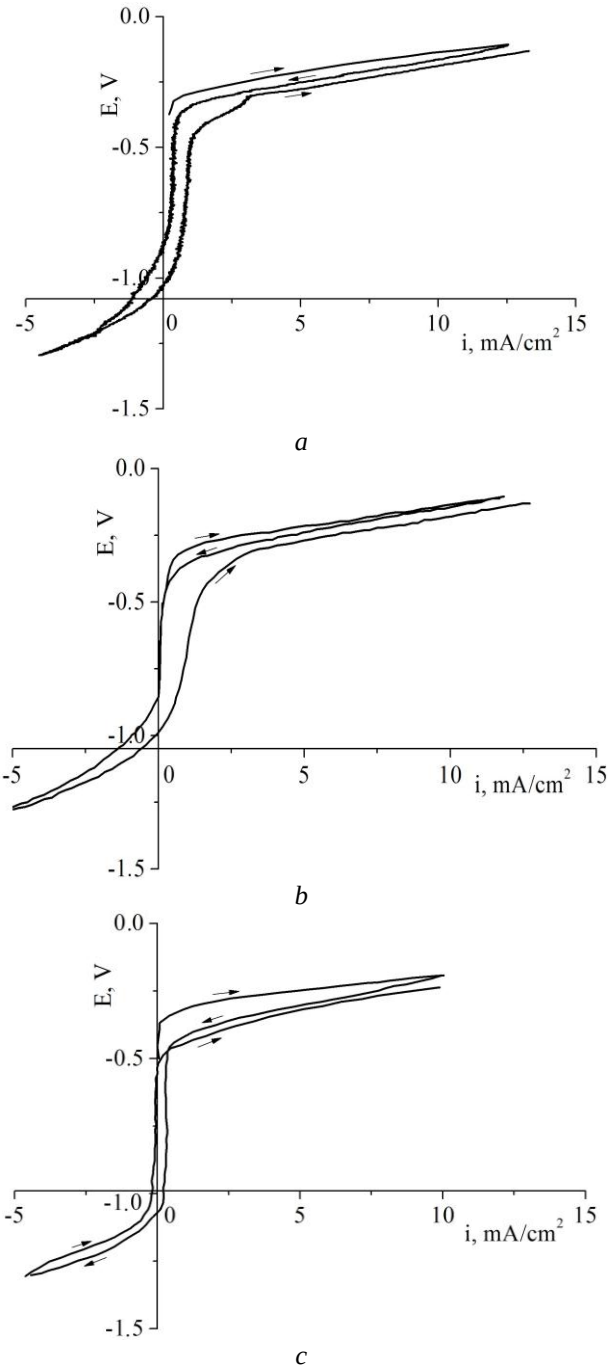

Fig. 4. Potential versus current curves of the corrosion in the NaCl solution (pH = 7) of the alloys: a – $Al_{72}Co_{18}Ni_{10}$; b – $Al_{65}Co_{20}Cu_{15}$; c – $Al_{72}Fe_{15}Ni_{13}$

Fig. 5 shows the SEM images of the surface of the studied alloys exposed to the NaCl aqueous solution for 8 days. On the corroded surface of the $Al_{72}Co_{18}Ni_{10}$ alloy, small pits sized about 10 μm are revealed (see Fig. 5,a). Pits, related to the microstructural heterogeneity, are located mainly in the vicinity of defects. Small pits do not remain active and relatively fast repassivation takes place. In addition to pitting, this alloy also shows a typical phase boundaries attack, i.e. preferential dissolution of the boundaries of crystalline $Al_9(Co, Ni)_2$ phase that contains more aluminum. However, such attacks occur only locally, resulting in

the lowest mass change and corrosion rate. The decagonal quasicrystals remain nearly unattacked even after the surrounding crystalline phases have corroded.

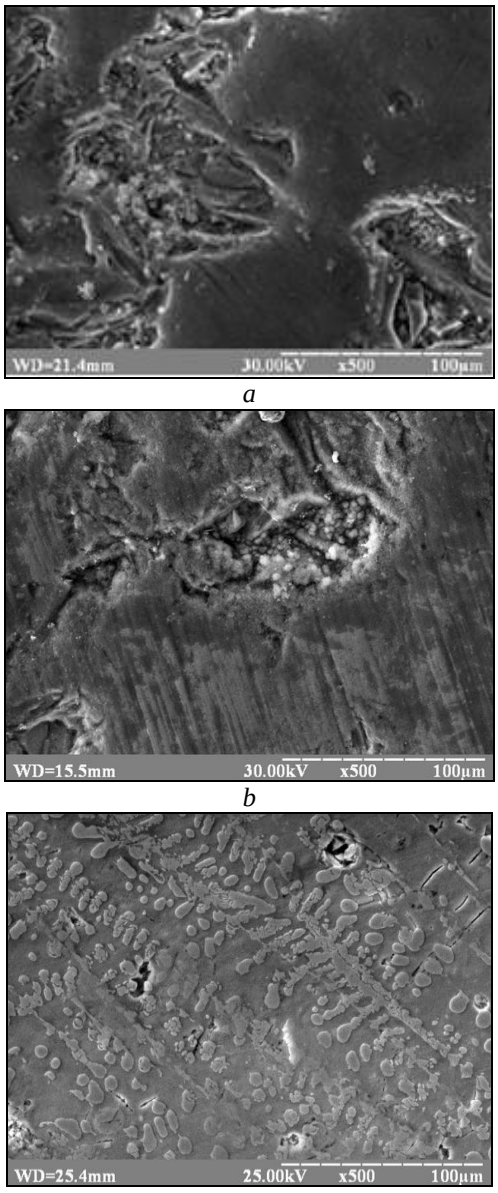

Fig. 5. SEM images of alloys' surface after staying for 8 days in the NaCl solution (pH=7): a – $Al_{72}Co_{18}Ni_{10}$; b – $Al_{65}Co_{20}Cu_{15}$; c – $Al_{72}Fe_{15}Ni_{13}$

Scanning electron microscopic investigations of the corroded surface of the $Al_{65}Co_{20}Cu_{15}$ alloy, evidence that pits ~ 10 μm in size are also observed (see Fig. 5,b). The corrosion attack is not uniform across the sample surface. The enhanced corrosion attack mainly occurs in crystalline $Al_3(Cu, Co)_2$ phase. The dissolution of the phase is most intense near its boundaries. This may be associated with the higher Al and Cu contents as compared with other phases of the alloy, making the $Al_3(Cu, Co)_2$ phase the most susceptible to attack and subsequent dissolution. Therefore, corrosion leaves small cavities along the phase boundaries. Meanwhile, Co-rich D-quasicrystals and crystalline $Al_4(Co, Cu)_3$ phase are less susceptible to corrosion.

The surface morphology of the $Al_{72}Fe_{15}Ni_{13}$ alloy indicates the presence of areas where corrosion, associated with pitting and/or selective dissolution, results in the formation of porous regions (see Fig. 5,c). Pits sites, sized from 5 to 20 μm, are distributed nonhomogeneously on the surface. The boundaries of crystalline Al_5FeNi phase enriched by iron are attacked more severely. This leads to phase boundary corrosion of the alloy, starting from the surface. D-quasicrystals are less prone to corrosion than the crystalline Al_5FeNi phase and stay almost uncorroded.

Thus, from the electrochemical point of view, the investigated alloys behave quite similarly in the aqueous sodium chloride solution but scanning electron microscopy shows that on the surface of the $Al_{72}Fe_{15}Ni_{13}$ alloy more corrosion-prone areas appear. So, the $Al_{72}Fe_{15}Ni_{13}$ alloy has the inferior resistance to pitting than the other alloys. The reason is that iron-rich phases and their boundaries in the structure of $Al_{72}Fe_{15}Ni_{13}$ alloy are more susceptible to attack by saline solution. On the contrary, corrosion of the $Al_{72}Co_{18}Ni_{10}$ alloy tends to progress least rapidly in the NaCl solution, little pit propagation takes place.

Generally, passive films formed on the surface of the studied alloys are susceptible to pitting corrosion that involves selective attack of the less noble alloys' constituents. The crystalline phases containing more iron or aluminum are preferentially dissolved when exposed to the NaCl solution. Accordingly, presence or formation of these phases should be avoided in the alloys applied in the marine climate. Whereas quasicrystalline D-phases react slowly and behave rather inert, especially those containing simultaneously Co and Ni, which are formed in the $Al_{72}Co_{18}Ni_{10}$ alloy that is only slightly pitted by saline solution. So, Co, and Ni are favorable for the corrosion resistance of the quasicrystalline alloys in the sodium chloride environment. These elements form a stable oxide layer on the alloy surface, blocking the diffusion of oxygen and so protecting it from corrosion.

CONCLUSIONS

The investigations performed on the conventionally solidified $Al_{72}Co_{18}Ni_{10}$, $Al_{65}Co_{20}Cu_{15}$, and $Al_{72}Fe_{15}Ni_{13}$ alloys confirm that all alloy systems cooled at 5 K/s form stable quasicrystalline decagonal D-phases.

Gravimetric and potentiodynamic measurements show that corrosion resistance of the $Al_{72}Co_{18}Ni_{10}$ alloy in the NaCl aqueous solution (pH = 7) is noticeably superior to that of the $Al_{65}Co_{20}Cu_{15}$ and $Al_{72}Fe_{15}Ni_{13}$ alloys. The corrosion proceeds by the electrochemical mechanism with oxygen depolarization. The alloys exhibit the formation of passive layer that blocks further dissolution. The passive film on the surface of the $Al_{72}Co_{18}Ni_{10}$ alloy shows best resistance to dissolution whereas it is poorest for the $Al_{72}Fe_{15}Ni_{13}$ alloy. On the corroded surface, the pits are revealed mainly where the crystalline phase boundaries and flaws are located. The D-quasicrystals are less susceptible to corrosion than crystalline phases containing more Fe or Al.

As compared with $Al_{65}Co_{20}Cu_{15}$ and $Al_{72}Fe_{15}Ni_{13}$ alloys, the improved corrosion characteristics of the $Al_{72}Co_{18}Ni_{10}$ alloy may be attributed to the content of

Co and Ni in its composition and thus favorable microstructure promoting the formation of most stable protective oxide film and reducing the extent of Al dissolution. This alloy has the less free corrosion potential, the lower corrosion current density, the broader electrochemical passivity region as well as scarcer and smaller pits on the surface affected by the saline solution. Therefore, the $Al_{72}Co_{18}Ni_{10}$ alloy shows promise as a starting material for plasma-sprayed coatings working in marine atmosphere.

REFERENCES

1. V.S. Sinyavskiy, V.S. Val'kov, V.D. Kalinin. *Corrosion and Protection of Aluminum Alloys*. M.: "Metallurgiya", 1986, 185 p.

2. Z.M. Stadnik. *Physical Properties of Quasicrystals*. Berlin-Heidelberg: "Springer-Verlag", 1999, 257 p.

3. H.R. Trebin. *Quasicrystals: Structure and Physical Properties*. Weinheim: "Wiley-VCH Verlag GmbH & Co.", 2003, 648 p.

4. E. Huttunen-Saarivirta. Microstructure, fabrication and properties of quasicrystalline Al-Cu-Fe alloys: a review // *Journal of Alloys and Compounds*. 2004, v. 363(1-2), p. 150-174.

5. S.M. Lee, H.J. Jeon, B.H. Kim, W.T. Kim, D.H. Kim. Solidification sequence of the icosahedral quasicrystal forming Al-Cu-Fe alloys // *Materials Science and Engineering*. 2001, v. A304-306, p. 871-878.

6. G. Rosas, J. Reyes-Gasga, R. Pérez. Morphology characteristics of the rapidly and conventionally solidified alloys of the AlCuFe system // *Materials Characterization*. 2007, v. 58(8-9), p. 765-770.

7. O.V. Sukhova, K.V. Ustinova. The effect of cooling rate on phase composition of quasicrystalline Al-Cu-Fe alloys doped with Si and B // *Functional Materials*. 2019, v. 26(3), p. 495-506.

8. E. Huttunen-Saarivirta, E. Turunen, M. Kallio. Influence of Cr alloying on the microstructure of thermally sprayed quasicrystalline Al-Cu-Fe coatings // *Intermetallics*. 2003, v. 11, p. 879-891.

9. A. Rudiger, U. Koster. Corrosion behavior of Al-Cu-Fe quasicrystals // *Materials Science and Engineering*. 2000, v. A294-296, p. 890-893.

10. E. Huttunen-Saarivirta, T. Tiainen. Corrosion behavior of Al-Cu-Fe alloys containing a quasicrystalline phase // *Materials Chemistry and Physics*. 2004, v. 85(2-3), p. 383-395.

11. O.V. Sukhova, V.A. Polonskyy. Peculiarities in structure formation and corrosion of cast quasicrystalline $Al_{63}Cu_{25}Fe_{12}$ and $Al_{63}Co_{24}Cu_{13}$ alloys in sodium chloride aqueous solution // *Physics and Chemistry of Solid State*. 2020, v. 21(3), p. 530-536.

12. I.M. Zhang, P. Gille. Solidification study of Al–Co–Cu alloys using the Bridgman method // *Journal of Alloys and Compounds*. 2004, v. 370(1-2), p. 198-205.

13. D. Holland-Moritz, G. Jacobs, I. Egry. Investigations of the short-range order in melts of quasicrystal-forming Al-Cu-Co alloys by EXAFS // *Materials Science and Engineering*. 2000, v. A294-296, p. 369-372.

14. K. Yubuta, K. Yamamoto, A. Yasuhara, K. Hiraga. Structure of an Al-Cu-Co decagonal quasicrystal studied by Cs-corrected STEM // *Materials Transactions*. 2014, v. 55(6), p. 866-870.

15. K. Edagawa, H. Tamaru, S. Yamaguchi, K. Suzuki, S. Takeuchi. Ordered and disordered phases in Al-Ni-Co decagonal quasicrystals // *Physical Review*. 1994, v. B50, p. 12413.

16. S. Hiramatsu, Y. Ishii. Theoretical prediction of phase diagrams for Al-Co-Ni decagonal quasicrystals // *Journal of the Physical Society of Japan*. 2006, v. 75(5), p. 054602.

17. L. Zhang, Y. Du, H. Xu, C. Tang, H. Chen, W. Zhang. Phase equilibria of the Al-Fe-Ni system at 850 °C and 627 °C // *Journal of Alloys and Compounds*. 2008, v. 454(1-2), p. 129-135.

18. K. Hiraga, K.T. Park. High resolution electron microscopy of Al-Ni-Fe decagonal quasicrystal // *Journal of Materials Research*. 1996, v. 11(7), p. 1702-1705.

19. Y. Zou, P. Kuczera, J. Wolny. Fitting the long-range order of a decagonal quasicrystal // *Acta Physica Polonica*. 2016, v. A130(4), p. 845-847.

20. B. Grushko, T. Velikanova. Formation of quasiperiodic and related periodic intermetallics in alloy system of aluminum with transition metals // *Computer Coupling of Phase Diagrams and Thermochemistry*. 2007, v. 31, p. 217-232.

21. Y. Lei, M. Calvo-Dahlborg, J. Dubois, Z. Hei, P. Weisbecker, C. Dong. Structure and morphology of [icosahedral $Al_{62}Cu_{25.5}Fe_{12.5}]_{100-x}$ [decagonal $Al_{70}Co_{15}Ni_{15}]_x$ alloys, for x=10*(0∼3 and 5∼10) // *Journal of Non-Crystalline Solids*. 2003, v. 330, p. 39-49.

22. Y. Zou, J.M. Wheeler, A.S. Sologubenko, J. Michler, W. Streurer, R. Spolenak. Bridging room-temperature and high-temperature plasticity in decagonal Al-Ni-Co quasicrystal by micro-thermomechanical testing // *Philosophical Magazine*. 2016, v. 96(32-34), p. 3356-3378.

23. A.P. Tsai, A. Inoue, T. Masumoto. Stable decagonal Al-Co-Ni and Al-Co-Cu quasicrystals // *Materials Transactions JIM*. 1989, v. 30(4), p. 300-304.

24. B. Grushko, K. Urban. A comparative study of decagonal quasicrystalline phases // *Philosophical Magazine*. 1994, v. B70(5), p. 1063-1075.

25. R. Wurschum, T. Troev, B. Grushko. Structural free volumes and systematics of positron lifetimes in quasicrystalline decagonal and adjacent crystalline phases of Al-Ni-Co, Al-Cu-Co, and Al-Ni-Fe alloys // *Physical Review*. 1995, v. B52(9), p. 6411.

26. S. Chen, T. Kuo, J. Liu, P. Lo, Y. Yen. Phase equilibria and wetting of Al-Co-Cu and Al-Co-Ni quasicrystals // *Materials Chemistry and Physics*. 2021, v. 263, p. 124409.

27. F. Nejadsattari, Z.M. Stadnik, J. Przewoznik, B. Grushko. Messbauer spectroscopy, magnetic and ab-initio study of the approximant $Al_{76}Ni_9Fe_{15}$ to a decagonal Al-Ni-Fe quasicrystal // *Journal of Alloys and Compounds*. 2016, v. 662(1-2), p. 612-620.

28. O.D. Neikov, S.S. Naboychenko, N.A. Yefimov. *Handbook of Non-Ferrous Metal Powders*. London: "Elsevier Ltd.", 2019, 973 p.

29. O.V. Sukhova. The effect of carbon content and cooling rate on the structure of boron-rich Fe-B-C alloys // *Physics and Chemistry of Solid State*. 2020, v. 21(2), p. 355-360.

30. A.D. Setyawan, D.V. Louzguine, K. Sasamori, H.M. Kimura, S. Ranganathan, A. Inoue. Phase composition and transformation behavior of rapidly solidified Al-Ni-Fe alloys in α-Al-decagonal phase region // *Journal of Alloys and Compounds*. 2005, v. 399(1-2), p. 132-138.

31. O.V. Sukhova. Structure and properties of Fe-B-C powders alloyed with Cr, V, Mo or Nb for plasma-sprayed coatings // *Problems of Atomic Science and Technology*. 2020, N 4(128), p. 77-83.

32. I.M. Zharskyy, N.P. Ivanova, D.V. Kuis, N.A. Svidunovich. *Corrosion and Protection of Metal Constructions and Equipment*. Minsk: "Vysheyshaya shkola", 2012, 303 p.

33. O.V. Sukhova, V.A. Polonskyy. Structure and corrosion of quasicrystalline cast Al-Co-Ni and Al-Fe-Ni alloys in aqueous NaCl solution // *East European Journal of Physics*. 2020, N 3, p. 5-10.

34. O.V. Sukhova, Yu.V. Syrovatko. New metallic materials and synthetic metals // *Metallofizika and Noveishie Technologii*. 2019, v. 41(9), p. 1171-1185 (in Russian).

35. O.V. Sukhova, V.A. Polonskyy, K.V. Ustinova. Structure formation and corrosion behaviour of quasicrystalline Al-Ni-Fe alloys // *Physics and Chemistry of Solid State*. 2017, v. 18(2), p. 222-227.

Article received 20.04.2021

СРАВНЕНИЕ КОРРОЗИИ В РАСТВОРЕ NaCl ДЕКАГОНАЛЬНЫХ КВАЗИКРИСТАЛЛОВ В СПЛАВАХ НА ОСНОВЕ АЛЮМИНИЯ

В.А. Полонский, Е.В. Суховая

Исследовали коррозионные свойства сплавов $Al_{72}Co_{18}Ni_{10}$, $Al_{65}Co_{20}Cu_{15}$ и $Al_{72}Fe_{15}Ni_{13}$, в структуре которых образуются декагональные квазикристаллы, в нейтральном растворе NaCl (pH = 7) с целью сравнения их коррозионной стойкости при эксплуатации в условиях морского климата. Микроструктуру сплавов изучали с помощью количественного металлографического, рентгеноструктурного, сканирующего электронно-микроскопического и микрорентгеноспектрального анализов. Коррозионные свойства определяли с использованием гравиметрического и потенциодинамического методов. Установлено, что сплавы $Al_{65}Co_{20}Cu_{15}$ и $Al_{72}Fe_{15}Ni_{13}$ сильнее корродируют в растворе натрий хлорида по сравнению со сплавом $Al_{72}Co_{18}Ni_{10}$. Коррозия, протекающая по электрохимическому механизму, сопровождается образованием пассивного поверхностного слоя, который препятствует растворению сплавов в солевом растворе после 3–4 суток испытаний. Метод сканирующей электронной микроскопии выявляет признаки питтинговой коррозии сплавов. Питтинги наблюдаются в местах расположения дефектов поверхности и границ кристаллических фаз, богатых на железо и алюминий. На поверхности сплава $Al_{72}Co_{18}Ni_{10}$ питтинги образуются в меньшем количестве и имеют меньшие размеры благодаря присутствию в его составе Co и Ni, определяющих скорость коррозионных процессов. Этот сплав может быть рекомендован в качестве стартового материала для плазменного напыления покрытий, эксплуатирующихся в условиях морского климата.

ПОРІВНЯННЯ КОРОЗІЇ В РОЗЧИНІ NaCl ДЕКАГОНАЛЬНИХ КВАЗІКРИСТАЛІВ У СПЛАВАХ НА ОСНОВІ АЛЮМІНІЮ

В.А. Полонський, О.В. Сухова

Досліджували корозійні властивості сплавів $Al_{72}Co_{18}Ni_{10}$, $Al_{65}Co_{20}Cu_{15}$ та $Al_{72}Fe_{15}Ni_{13}$, у структурі яких утворюються декагональні квазікристали, в нейтральному розчині NaCl (pH = 7) з метою порівняння їх корозійної стійкості під час експлуатації в умовах морського клімату. Мікроструктуру сплавів вивчали за допомогою кількісного металографічного, рентгеноструктурного, сканувального електронно-мікроскопічного та мікрорентгеноспектрального аналізів. Корозійні властивості визначали із застосуванням гравіметричного та потенціодинамічного методів. Встановлено, що сплави $Al_{65}Co_{20}Cu_{15}$ та $Al_{72}Fe_{15}Ni_{13}$ сильніше кородують у розчині натрій хлориду порівняно зі сплавом $Al_{72}Co_{18}Ni_{10}$. Корозія, яка відбувається за електрохімічним механізмом, супроводжується утворенням пасивного шару на поверхні, який запобігає подальшому розчиненню сплавів у сольовому розчині після 3–4 діб випробувань. Метод сканувальної електронної мікроскопії виявляє ознаки пітінгової корозії сплавів. Пітінги спостерігаються в місцях розташування дефектів поверхні та границь кристалічних фаз, багатих на залізо та алюміній. На поверхні сплаву $Al_{72}Co_{18}Ni_{10}$ пітінги утворюються в меншій кількості та мають менші розміри завдяки присутності в його складі Co та Ni, що визначають швидкість корозійних процесів. Цей сплав може бути рекомендований як стартовий матеріал для плазмового напилення покриттів, які експлуатуються в умовах морського клімату.